PHILIPPINE ENGINEERING JOURNAL
PEJ 2024; Vol. 45, No. 1: 29-56

Received: 01 September 2023
Accepted: 05 May 2024

Modelling the Sediment Dynamics of a Developing Coastal Estuary: The Case of Batan Bay, Aklan

Franz D. Santos[1,2,*], Eugene C. Herrera[1,2], Bryan Clark B. Hernandez[2], Gene Euclid T. Dela Cruz[2], Francois Hanz Detriech M. Almarza[2], Ryan M. Basina[3], Masaya Yoshikai[4], and Kazuo Nadaoka[4]

[1] Institute of Civil Engineering, University of the Philippines, Diliman, Quezon City, 1101, Philippines
[2] National Hydraulic Research Center, University of the Philippines, Diliman, Quezon City, 1101, Philippines
[3] College of Fisheries and Marine Sciences, Aklan State University, New Washington, Philippines
[4] School of Environment and Society, Tokyo Institute of Technology, Tokyo, Japan
Corresponding author: fdsantos@up.edu.ph

Abstract *– In most coastal communities, aquaculture has been the way to address the continuous urbanization and growth in population in these areas. Aquaculture has proven to be economically important, but mismanagement of the coastal resource has often led to decline in productivity. Batan Bay Estuary in Aklan has been experiencing lower productivity and shallower bay waters over years of urbanization and thriving aquaculture activities. Given the limitation of actual data gathering techniques to represent physical processes of water bodies such as estuaries, numerical modelling has been used as a tool to describe estuarine processes as well as aid in the management and preservation of its different ecosystem services. This study aimed to describe and understand the sediment dynamics of Batan Bay Estuary using numerical modelling. Sediment yields were simulated using the Soil and Water Assessment Tool+ (SWAT+) to describe the long-term hydrology while Delft3D was utilized in understanding the hydrodynamics and sediment dynamics of the bay. Based on the morphologic simulation results, erosion areas were identified at the narrow channels between fishpond dikes while sediment deposition areas were identified at fishpond dike entrances and near the bay mouth. A scenario for bay management such as removing abandoned fishpond dikes in the bay and its effects on the sediment dynamics was also examined. Simulation showed that areas near the removed dikes resulted in an increase in velocity by as much as 0.5 m/s thus resulting in more erosion near these areas. The results generated from the models can aid the community in understanding the effects of future aquaculture developments on the sedimentation dynamics of the bay. This study has shown the value of utilizing advanced numerical modelling techniques and data analysis in understanding sediment dynamics of coastal resource and effectively come-up with scientific-based information to support bay-wide conservation and resource-use efforts.*

Keywords*: aquaculture, Deflt3D, numerical modelling, sediment dynamics, sustainability*

I. INTRODUCTION

Rapid increase in population for coastal regions have been observed in many developing countries including the Philippines. Along with the continuous increase in inhabitants is an increase in the demand for food and livelihood of people residing in coastal communities. The significance of fisheries and aquaculture in providing food, nutrition as well as employment across the world has gained more attention in the past decade. Throughout the years, activities related to aquaculture has been increasing and regarded as one of the fastest-growing food industries worldwide [1] with Asia being a dominant contributor in the fish farming industry generating 90% of the total global aquaculture volume with pond systems located in fertile coastal environments [2].

The position of coastal zones and circulation patterns from fresh and saltwater interaction makes these regions effective sediment traps. Hydrodynamics and saltwater intrusion in the estuaries are complex three-dimensional processes and are driven by both natural and anthropogenic factors [3]. The sediment fluxes and budgets, on the other hand, are essential for both estuarine and coastal environments [4] and are the result of interplay between freshwater inflow, tidal currents, wind-wave resuspension, commercial fishing, and dredging operations [5]. Naturally, the rate of sediment accumulation in estuaries are high due to its multiple drivers such as flow velocities, tides, current, and sediment loads coming from upstream; but due to the anthropogenic activities and presence of coastal structures that affect bay hydrodynamics, this rate has evidently increased. Erosion and deposition of sediments are determined by the interchange between hydrodynamic conditions and sediment properties [6]. In the sustainable management of coastal areas, proper understanding of its hydrodynamics and sediment dynamics is essential [7]. Insights on the behavior of these dynamic systems are needed to evaluate current conditions as well as simulate future development under natural forcing as well as man-made alterations [8]. To understand these movements, numerical models are often used for engineering purposes in estuarine areas [9]. These numerical models are used to assess and describe the effect of each forcing and to represent the dynamic process of estuaries accurately [10]. Given the limitation of actual data gathering techniques when it comes to representing physical processes of water bodies, numerical modelling can also be utilized as a tool to approximate mathematical equations that describe estuarine and coastal processes as well as the fate and transport of sediments.

In a study conducted by Cheng et al. [11], the Finite Volume Coastal Ocean Model (FVCOM) - a 3D hydrodynamic model – was used to explore the hydrodynamic changes after land reclamation in the Yalu River Estuary in China. Wang & Andutta [12] on the other hand discussed analyzed the effect of dike construction on sediment transport in Yangtze River Delta using the Princeton Ocean Model (POM) as a modelling platform. Results of the simulation considering the dikes showed that the maximum suspended sediment concentration (SSC) was observed adjacent to the north dike and in contrast, simulation without the dikes showed that high SSC was found in the entire area near the estuarine mouth. The Coupled Ocean–Atmosphere–Wave–Sediment Transport (COAWST) is a modelling system that accounts for the combined current and wave stresses and accretion of sediments through suspended and bedload transport [13]. COAWST has been used to describe the influence of submerged vegetation patches on currents for a shallow basin [14] and has also been utilized to demonstrate multiple-bed model for the morphological modelling of different sediment classes that considers vertical exchange or settling with the bed [15].

Delft3D is a modelling suite that has different modules that simulates hydrodynamic flow, transport of constituents such as salinity and heat, and transport of sediments and the consequent morphological changes [16]. This state-of-the-art modelling software has been successfully used in describing hydrodynamic and sediment transport characteristics of rivers, estuaries, and coastal environments. It has proven its effectivity in determining the effects of longshore currents to the longshore transport and its correlation to the design of non-tidal beaches [17]. In the Nile River in Egypt, Delft3D has also been utilized in determining the impact of a waterfront development project on river hydraulic properties [18]. Sediment transport patterns during flood and storm events that occurred between 1979 and 2010 on Rhone Delta at the Mediterranean Sea were also studied using Delft3D [19]. In addition, a coupled Delft-FLOW and sediment transport model was used in a study conducted by Tu et al. [20] to investigate the effects if salinity, winds, and tides on sediment transport in the estuary of the Vietnamese Mekong Delta.

Batan Bay Estuary in Aklan, Philippines is known for its very productive aquaculture, abundant mangrove forests and diverse aquatic resources. Over years of urbanization and thriving aquaculture activities, it been experiencing lower aquaculture productivity and shallower bay waters. There are papers that discussed the history of aquaculture development in Batan Bay along with the declining trends in productivity but there has not been any study that described the hydrodynamics and sediment dynamics of the bay using numerical modelling. This paper aimed to describe and understand the sediment dynamics of Batan Bay using numerical modelling. Hydrologic, hydrodynamic, and sediment dynamics models were set-up and utilized in this study and were calibrated using observed data from intensive field surveys. The modelling platforms that are mentioned in the next sub-section were used generate useful information for to be used for policy making and management of water resources. But considering the accessibility, ease, and availability of user manuals to maximize the use of numerical modelling software, this study utilized Delft3D. Aside from these reasons and more importantly, Delft3D has also proven its accuracy and robustness for describing nearshore conditions [21].

II. METHODOLOGY

2.1 The Study Site

Batan Estuary (11°35’N and 122°29’E) is a semi-enclosed estuarine system composed of lagoons and rivers with a total water area of 2640 hectares. Located on the northern part of Panay Island in Western Visayas, the bay caters freshwater from the inland area through the Camaligan and Jaro Rivers and saline water coming from the Sibuyan Sea as shown in Figure 1.

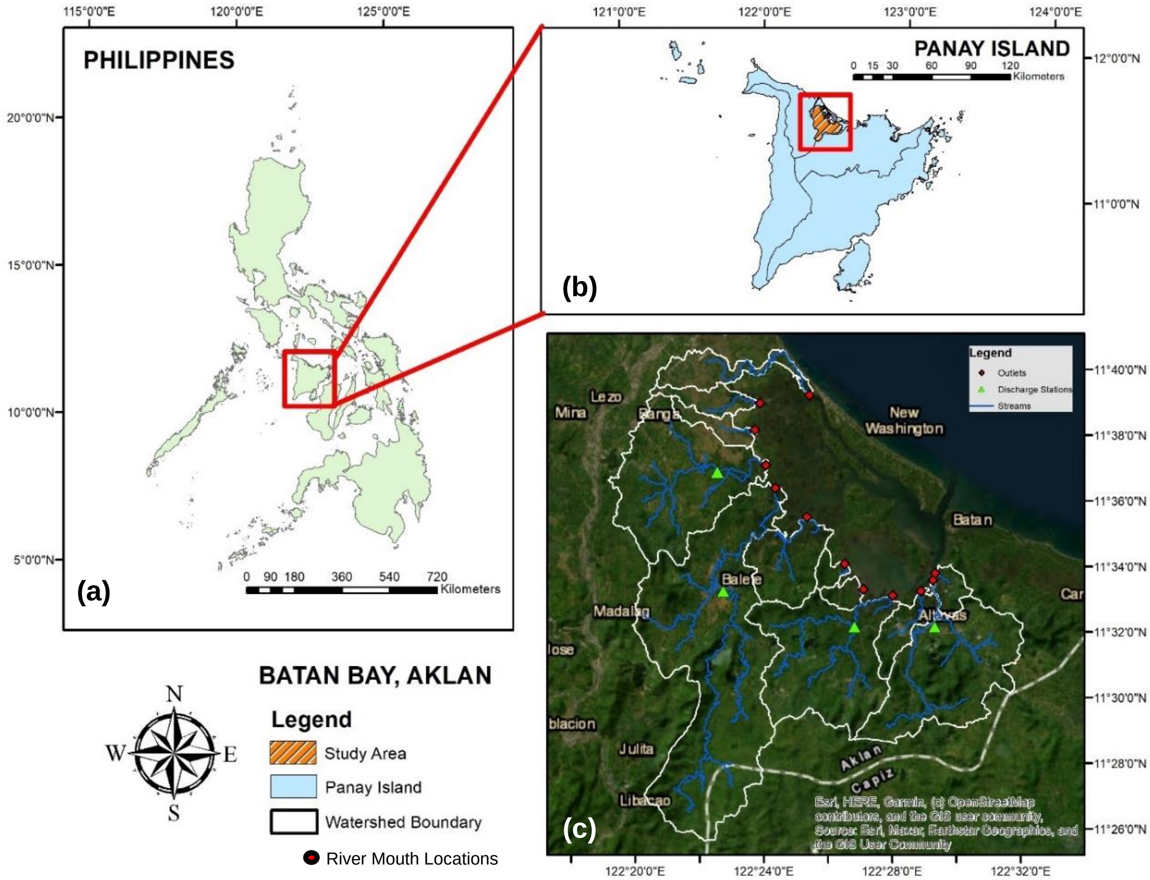

Figure 1. Study Area in Batan Bay, Aklan (a) Philippine Map, (b) Panay Island, and (c) Boundary of Batan Bay Watershed showing major tributaries, outlets, and discharge locations.

Batan Bay was known for its very productive aquaculture, abundant mangrove forests and diverse aquatic resources. The upsurge in number of aquaculture ponds intensified to compete with the growing demand of fish production. As a result, majority of the mangrove forests had been converted to fish and shrimp ponds [22] thus causing the area to suffer from degrading environment and decline in aquaculture productivity [23].

Moreover, through the years the dominant land covers in the Batan watershed such as agricultural lands, range lands (grasslands and shrublands), and built-up areas were observed to dynamically change because of continuous development and growth in population in the area. Decadal land cover maps (1990 to 2020) that were derived from remote sensing under the Comprehensive Assessment and Conservation of Blue Carbon Ecosystems and their Services in the Coral Triangle (BlueCARES) Project were processed using GIS to determine the percentage per land cover based on the total basin area. Depicted in Figure 2 is the decadal land cover trend of Batan Bay watershed showing the changes over three decades.

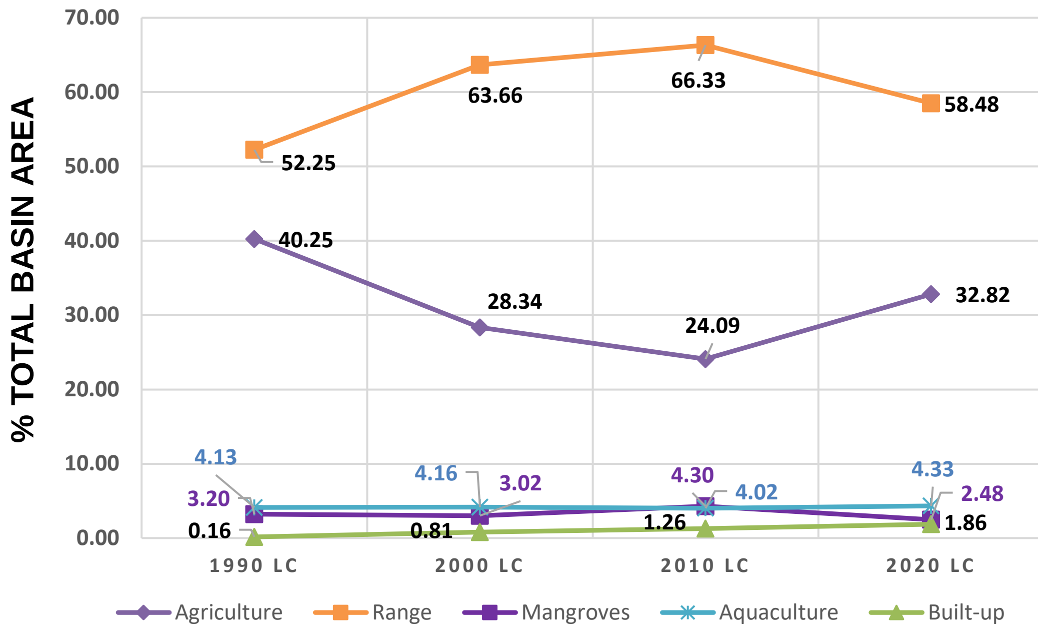

Figure 2. Decadal Land Cover Trend of Batan Bay Watershed

The land cover of Batan Bay is dominated by agricultural areas in the year 1990 that happen to decrease up to the year 2010 and increase toward 2020. Increase in rangelands (shrublands and grasslands) can be observed from year 1990 to 2010 and was observed to decrease moving toward 2020 while built-up areas were progressively increasing from 1990 to 2020. Aquaculture areas has shown a decrease in 2010 but was generally increasing from 1990 to 2020. These changes in land cover could contribute to the changing sediment yields coming from the watershed that is discharged to the bay area.

2.2 Data Gathering and Field Observation

Primary and secondary data were obtained from intensive field surveys while other data sets were requested from government agencies for this study. Topographic Data such as the digital elevation model and land cover were requested both from the National Mapping and Resource Information Authority (NAMRIA) and from Comprehensive Assessment and Conservation of Blue Carbon Ecosystems and their Services in the Coral Triangle (BlueCARES) Project. The digital topography of Batan Bay that was used for this study was a Digital Terrain Model (DTM) obtained from NAMRIA. It was a 5-m resolution product of Interferometric Synthetic Aperture Radar (IfSAR), one of the fastest growing technologies in providing satisfactory resolution DEMs according to [24]. These satisfactory to high resolution DEMs often produce accurate results thus being most preferred data sets in hydrologic modelling [25]. The land cover maps on the other hand were outputs from remote sensing of the BlueCARES Project.

In setting up the hydrology model of the study area, long-term meteorologic data were requested by the proponent from Philippine Atmospheric, Geophysical and Astronomical Services Administration (PAGASA) and Department of Science and Technology Advanced

Science and Technology Institute (DOST-ASTI) while a weather station was also set-up in Aklan during the data gathering stage. Data inputs for the hydrodynamic model such as bay bathymetry was requested from the BlueCARES Project repository while fishpond depths were obtained by performing fishpond bathymetry survey in April and October of 2022. In addition, ocean data for the long-term model simulation were downloaded from available online ocean model outputs such as Hybrid Coordinate Ocean Model (HYCOM) (https://www.hycom.org/, last accessed 20 June 2023) and ocean global data sets of the National Center for Environmental Information (NCEI) (https://www.ncei.noaa.gov/, last accessed 18 April 2023). Shown in Figure 3 is the bathymetry of the study area. The uniform depths within the inner bay area are the fishpond areas bounded by dikes depicted by black boundaries in the domain.

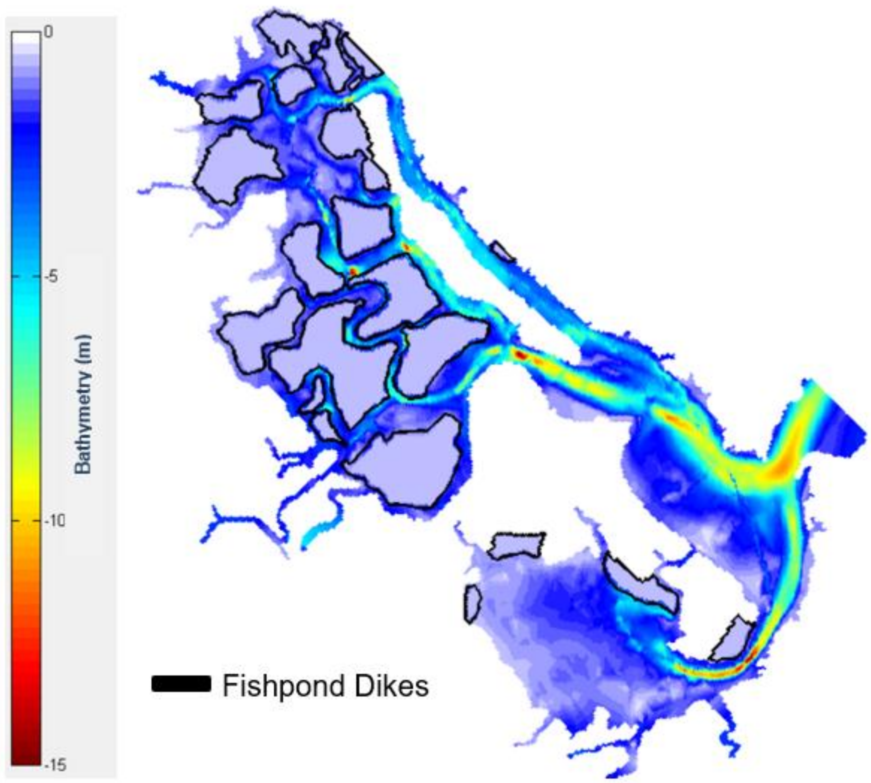

Figure 3. Bathymetry and Batan Bay Estuary Boundary Showing Fishpond Dikes

During the June 2019 field survey, sensors were deployed at different locations of Batan Bay to measure different hydrodynamic parameters. For one tidal cycle, the Water level was measured in 10-minute intervals using a water level logger while the ACTW digital output cable sensor was utilized to measure salinity in 15-minute intervals. Velocity magnitudes was also measured every 30 minutes near bottom surface using an EM meter. Shown in Figure 4 are the locations of deployed sensors in Batan Bay.

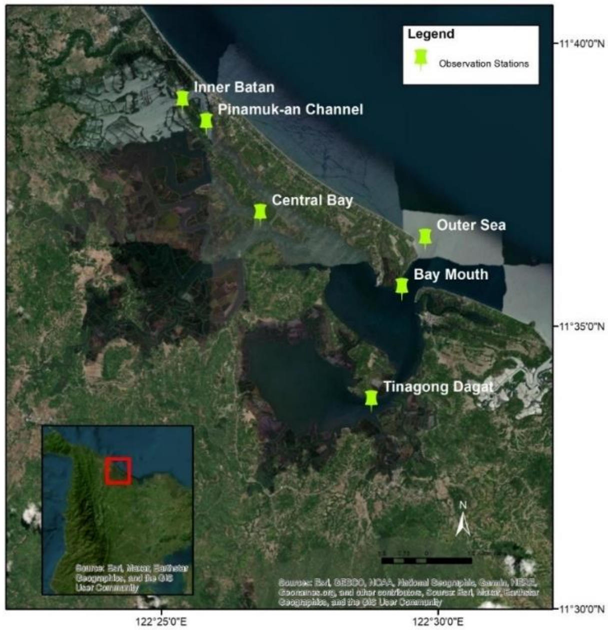

Figure 4. Hydrodynamic Sensor Deployment Locations

Sediment properties were needed as input in the numerical model but due to unavailability of field measurements, data on characteristics of estuarine sediments from various literatures were adopted in addition to some sediment properties as given in the Delft3D Manual. Properties of median sediment diameter for sand and silt as well as settling velocities for clay were used as inputs for the sediment dynamics set-up. Table 1 summarizes the sediment data inputs that were used in setting up the sediment dynamics model.

Table 1. Sediment Data Inputs

Sediment	Data	Value	Reference
Sand	Specific Density	2650 kg/m^3	[26]
	Sediment Diameter	200 mm	**[27]**
Silt	Specific Density	2160 kg/m^3	[28]
	Sediment Diameter	64 mm	[29]
Clay	Settling Velocity	0.76 mm/s	[30]

2.3 Numerical Modelling

As this paper intends to describe and understand the sediment dynamics of the study area after collection of both primary data and secondary data from government agencies, intensive field surveys, and online databases in the data gathering data gathering phase, the use of numerical models to simulate watershed and bay conditions was performed.

2.3.1 Hydrology

SWAT+, an improved version of the Soil and Water Analysis Tool (SWAT) was utilized for modelling the hydrologic response and sediment yield of Batan Bay Watershed. SWAT+

is a plug-in for QGIS, a GIS software that has been found reliable for applications in water resource management [31] and is termed as QSWAT+. Delineation in QSWAT+ uses the topography of the DTM to divide the watershed into different subbasins. For each subbasin, one reach is defined to it with that drains to an outlet at the downstream part of the subbasin. After watershed delineation, inputs of land cover, soil type, and slope class are needed to define the hydrologic response units (HRUs) that are the smaller units of the watershed where hydrologic processes are executed. Meteorologic data such as rainfall, temperature, wind, and solar radiation that were acquired from government agencies and from the weather station deployed during field survey were used as inputs in setting up the watershed model.

A five (5) year hydrology simulation (including two years warm-up period) at daily time steps was done to describe the watershed flow regime and sediment generation. In quantifying the sediment runoff in the watershed, the Modified Universal Soil Loss Equation (MUSLE) which uses rainfall as driver for erosion and utilizes the amount of runoff to simulate erosion and sediment yield was utilized. Outputs of discharge and sediment yield from the watershed were then used as inputs to Delft3D.

2.3.2 Hydrodynamics

The computational grid shown in Figure 5 that represents Batan Bay was created using RFGRID, the built-in program of Delft3D for grid generation and editing. It intends to create grids at minimal efforts that meets requirements of smoothness and orthogonality [32].

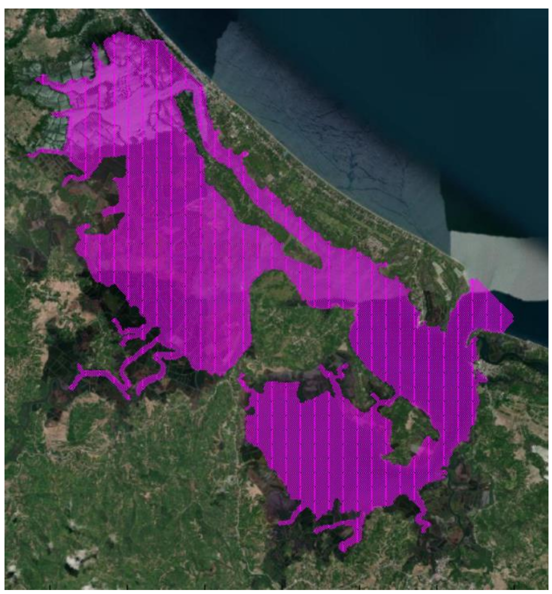

Figure 5. Hydrodynamic Model Set-up

The domain of the created grid covers Batan Bay including channels between fishponds, Pinamuk-an channel, and Tinagong Dagat. The grid is made up of 237 x 386 grid points at 20 meters from each other. Computational domain was composed of three (3) layers at 33.33% of the depth each. Creating the model domain in three dimensions make it possible to analyze hydrodynamic parameters near-bottom of the bay. Fishpond dikes were represented by “thin dams”, structures in Delf3D that allows water to flow around it but does not allow exchange between adjacent grid cells without reducing the volume of the model [26]. Thin dams were placed outlining the fishpond dikes leaving one face of the grid cell open to allow exchange from the bay.

An open boundary was defined at the Bay mouth where the time-series water level from field surveys as well as those requested from NAMRIA to complete the one-year period were applied. Transport conditions of salinity and temperature at the open boundary were time-series data downloaded from online global ocean model outputs such as Hybrid Coordinate Ocean Model (HYCOM) and global data sets of the National Center for Environmental Information (NCEI). To model the heat exchanges between the atmosphere and water bodies, a heat flux model was defined for the hydrodynamic model. There are many methods available in modelling heat flux and they differ in dependency of exchange based on meteorologic characteristics such as wind speed, cloud cover, and humidity. For this research, the Murakami Heat Flux model that computes effective back radiation and heat losses due to evaporation and convection [26] where daily meteorologic time-series data of relative humidity, solar radiation, and air temperature were used as inputs.

A one-year simulation was done to describe seasonal variation in hydrodynamics covering both wet and dry seasons. Batan Bay is an estuary exchanging waters with the sea and thus, prevailing wind that vary with the seasons play an important factor in bay hydrodynamics and consequently in the transport of sediments.

2.3.3 Sediment Dynamics

The Morphodynamic modelling module of Delft3D was utilized for the sediment dynamics part of the study. Results of the hydrodynamic model were coupled with the results of the sediment transport model as shown by the two-way arrow to capture and incorporate morphodynamic changes such as bathymetry updating in the calculations during the simulation. An equilibrium boundary condition at the mouth was defined for the sediment model. Following the equation of Van Rijn [33] for the transport of sediments, the equilibrium boundary condition implements that at the open boundaries, the flow enters carrying the same concentration of sediments as computed in the interior of the model. Moreover, since sediment concentrations adapt to equilibrium conditions quickly in many practical applications, a uniform zero concentration is typically sufficient during cold starts when the hydrodynamic model also takes some time to stabilize [26].

After all simulation works, an analysis of the flow regime and sediment yields of the watershed, along with hydrodynamics and sediment transport dynamics of Batan Bay was performed. Shown in Figure 6 is the summarized modelling framework of this study

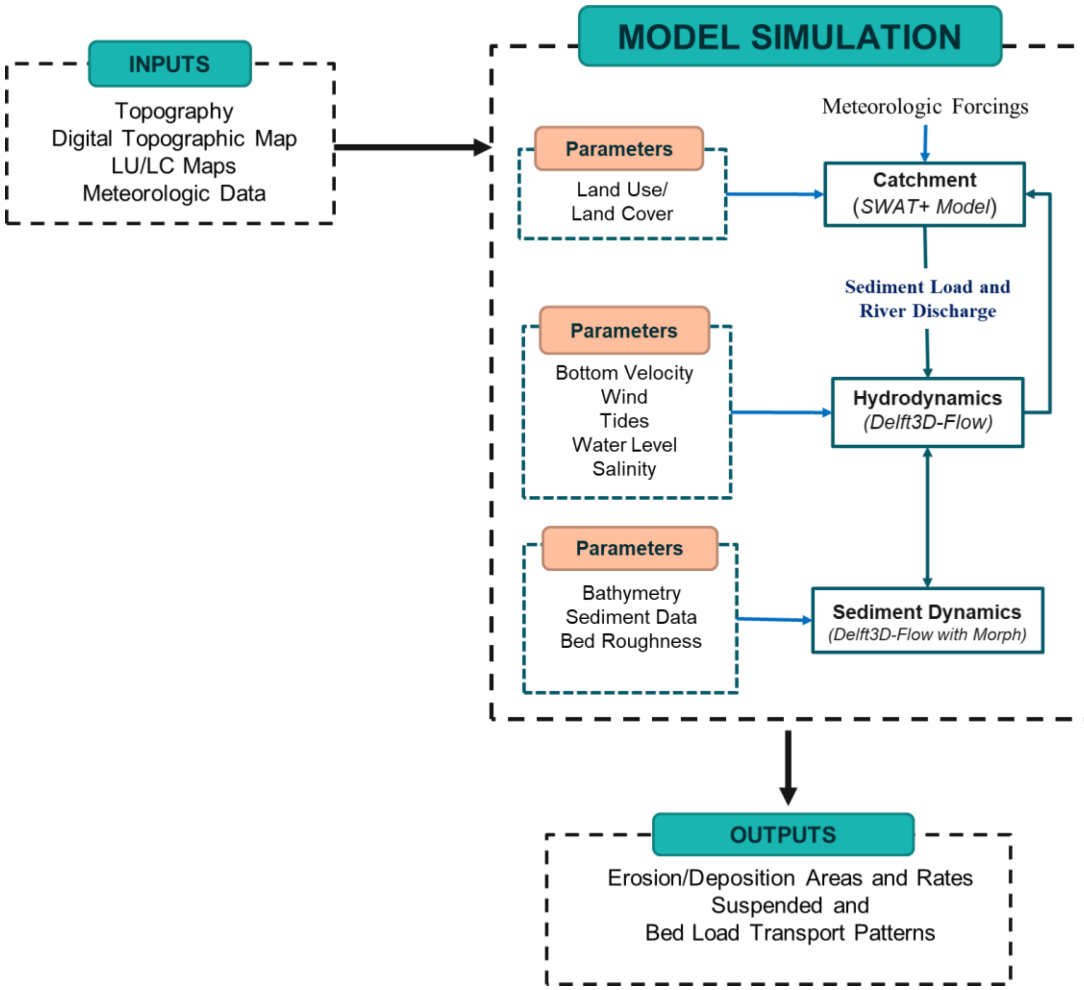

Figure 6. Modelling Framework

2.4 Model Calibration

Measurement of model accuracy was done by determining the level of agreement between simulated and measured data using the root-mean-square-error (RMSE). The RMSE measures the deviation of the residuals from the regression line or describes how concentrated is the data to the best fit line. Lower values of RMSE are desired since it indicates less residual variance and better model performance [34]. RMSE is given by the equation:

$$RMSE = \sqrt{\frac{1}{n}\sum_{i=1}^{n}(S_i - O_i)} \qquad (1)$$

where Si: simulated output
Oi: observed data
n: number of observations.

In addition, the Nash-Sutcliffe Efficiency (NSE) which measures residual variance to measured standard variance [35] was used in the calibration of the watershed model. The NSE can be computed by evaluating the observed (O), average observed ($\bar{O}$) and predicted (P) values as shown:

$$NSE = 1 - \frac{\sum_{i=1}^{n}(O_i - P_i)^2}{\sum_{i=1}^{n}(O_i - \bar{O})^2} \tag{2}$$

According to [35], in terms of the NSE as a parameter to assess model performance, NSE values of greater than 0.50 up to 0.70 for daily calibration was satisfactory. A good model rating is given for values of NSE greater than 0.70 up to 0.80 while NSE values of less than 0.50 means unsatisfactory. Another statistical parameters that were used to measure the agreement or mismatch between observed and model predicted data is the Pearson's Correlation Coefficient (R) which is computed using the equation:

$$R = \frac{\frac{1}{n}\sum_{i=1}^{n}(S_i - \bar{S_i})(O_i - \bar{O_i})}{\sqrt{\sum_{i=1}^{n}(S_i - \bar{S_i})^2}\,\sqrt{\sum_{i=1}^{n}(O_i - \bar{O_i})^2}} \tag{3}$$

where Si: simulated output
$\bar{S_i}$: mean of all simulated outputs
Oi: observed data
$\bar{O_i}$: mean of all observed data
n: number of observations.

A value of unity indicates that the observed and simulated data have perfect correlation while R values greater than 0.50 signify moderate to strong correlation between the data [36].

2.5 Model Scenario: Removing Abandoned Fishponds

After model calibration, the hydrodynamics, sediment transport characteristics, and effects on the morphology of sedimentation processes were described. After which, the calibrated hydro-sediment model of Batan Bay was then used to simulate a scenario to test possible bay management schemes through model application. Removal of abandoned fishponds from the bay was done to assess its effects on both the hydrodynamics and the sediment dynamics of the study area.

III. RESULTS AND DISCUSSION

3.1 Model Calibration

3.1.1 Hydrology Model Calibration

The outlet discharges from the SWAT+ model was used as inputs to Delft3d-FLOW. Data on bay salinity were used to calibrate results of the hydrologic model due to the lack of sufficient measured river discharge data. The process was iteratively done until the model simulated and observed salinity reached a best-fit set-up. Resulting discharges after the last iteration for salinity balance were extracted and was used to calibrate the hydrology model.

After the calibration process, flows from Jal-O River, the stream found in the largest subbasin of the watershed were plotted to get the statistical parameters for assessment of model accuracy. Shown in Figure 7 is the calibration plot of Jal-O River.

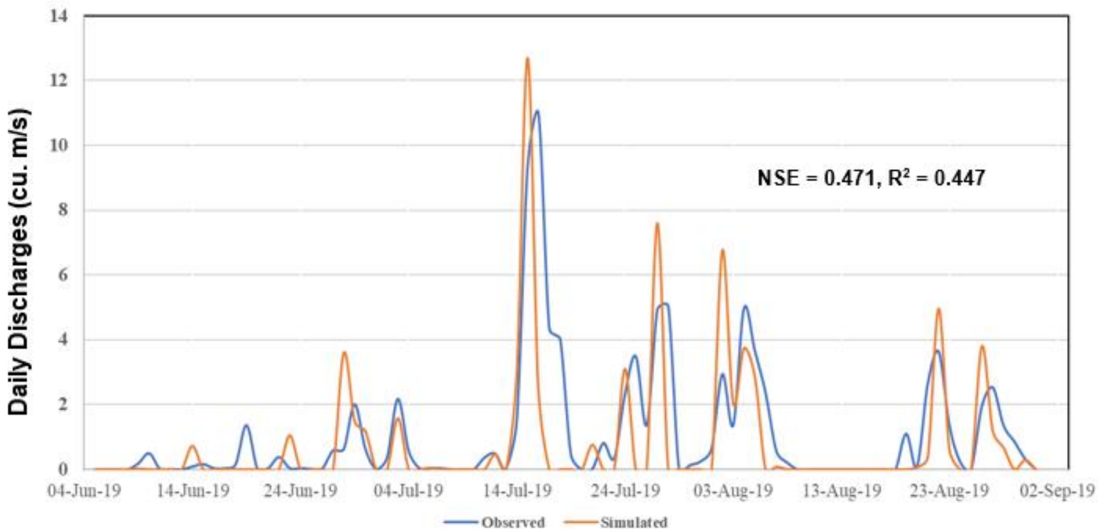

Figure 7. Jal-O River Daily Flow Calibration

The value of the Nash-Sutcliff Efficiency (NSE) was computed after calibration and it was near the satisfactory value of 0.50. Due to the lack of available discharge data in the study area, the freshwater discharges of the watershed model were calibrated and the resulting salinity from the hydrodynamic model was compared to measured salinity at the different observation points within the bay. Moreover, lower performance rating could be attributed to the limited available monitoring stations within the basin [37].

Another major tributary in Batan Bay is the Talon River where the subbasin containing it is in the municipality of Altavas. Its outlet is discharging in Tinagong Dagat and was also subjected to calibration. Shown in Figure 8 is the calibration of Talon River.

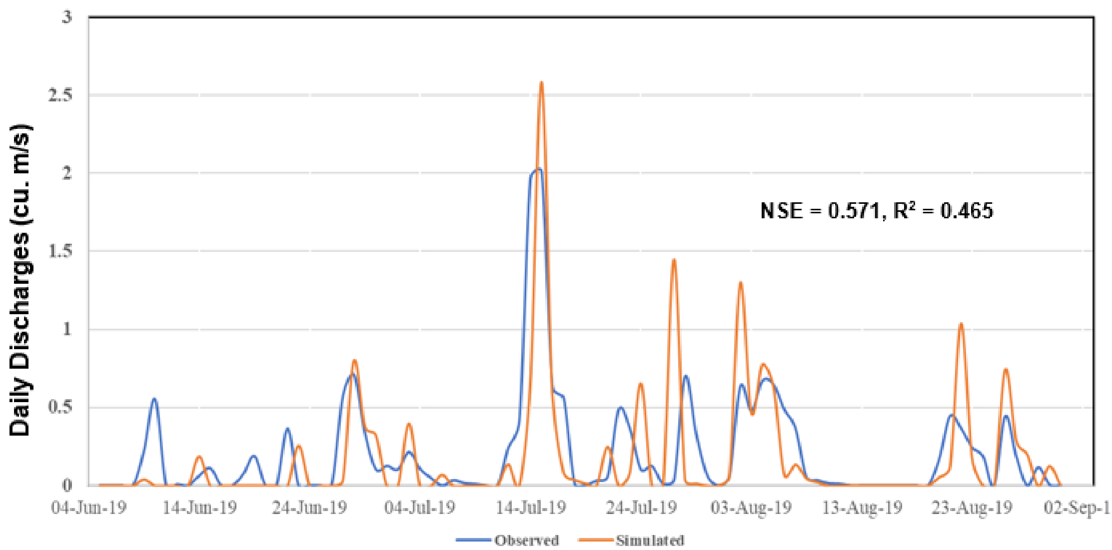

Figure 8. Talon River Daily Flow Calibration

From the results of calibration, the NSE has reached satisfactory rating at 0.571 however the R^2 still fell short of the satisfactory target of 0.50. The NSE value for this subbasin recorded a higher value as compared to that of the Balete Subbasin which may be attributed to the basin size. Since the Balete subbasin is the largest subbasin in terms of drainage area and could be expected to deliver larger runoff volumes to the stream. Moreover, the availability of a gauging station in the basin could have also improved these statistical parameters.

3.1.2 Hydrodynamic Model Calibration

Before performing a long-term hydrodynamic and sediment dynamic model simulation, the water level and salinity parameters were calibrated using observed data from the June 2019 field survey. The results of model calibration are presented below.

3.1.2.1 Water Level

Sensitivity analysis was performed to evaluate the parameters that would influence the water level in the bay, however an iterative process of varying the different physical parameters did not result in any significant change in the water level variations. This phenomenon can be credited to the bay being dominated by strong tidal forcings. Observed and simulated water levels at a monitoring station near the bay mouth are shown in Figure 9. RMSE values range from 0.035 m to 0.15 m indicating good prediction capability of the model.

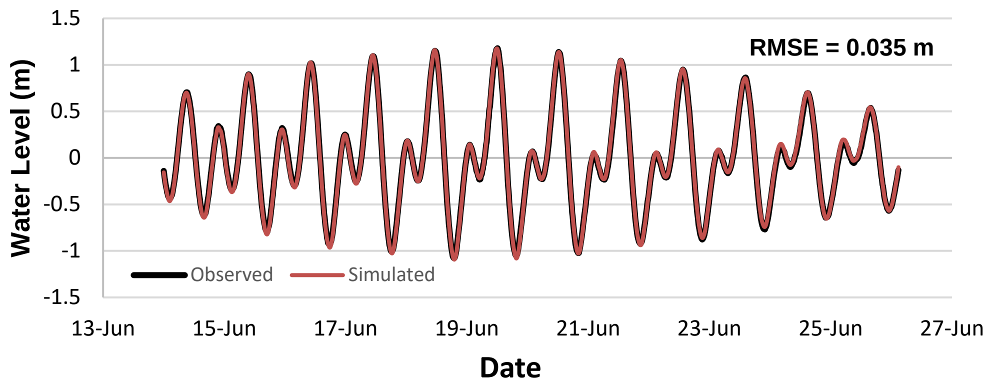

Figure 9. Simulated and Observed Water Levels at Bay Mouth after Calibration

3.1.2.2 Salinity

Observed data on bay salinity were used to calibrate results of the hydrologic model because of the lack of sufficient measured river discharge data. Calibrated discharges were then used as input in the hydrodynamic model to validate the salinity outputs. Shown in Figure 10 are the results of salinity calibration using the flows from the calibrated watershed model for one of the observation stations within the bay. The salinity values are from a station within the inner bay area located at Pinamuk-an Channel. Values of the correlation coefficient for all observation stations range from 0.51 to 0.91 which indicates that the simulated and observed salinity are moderately to strongly correlated.

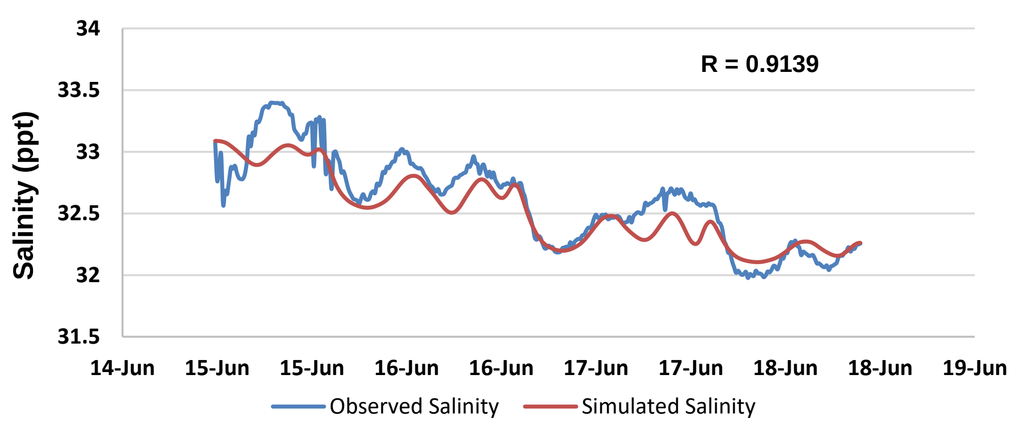

Figure 10. Model Simulated and Observed Salinity at Pinamuk-an Channel after Calibration

3.1.2.3 Bottom Velocity

Velocity is an important parameter to consider in describing the transport of sediments in water bodies. For this reason, after completing water level calibration, model simulated velocities were compared to observed near-bottom velocities. Sensitivity analysis was again performed to determine the parameters that would influence velocity variations. It was found out from the iterative process that the velocity magnitude is greatly affected by the bottom roughness (Manning's roughness as used in this research), that is, greater bed roughness values applied to the computational domain tend to produce lower velocity magnitudes and lower values of bed roughness tend to produce higher magnitudes of velocity. Shown in Figure 11 are the results of velocity calibration using the flows from the calibrated watershed model for an observation station located in Pinamuk-an Channel.

To assess model performance, the Pearson's Correlation Coefficient was utilized in this study. For both magnitude and direction, values of R ranged from 0.51 to 0.73 indicating moderately to strong correlation between simulated and observed data.

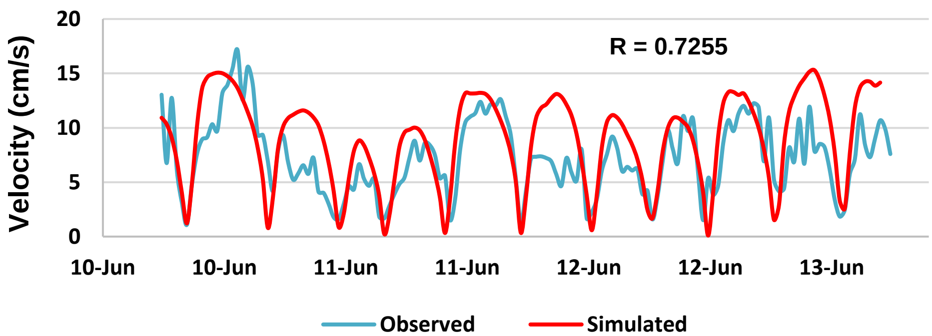

Figure 11. Model Simulated and Observed Velocity at Pinamuk-an Channel after Calibration

3.2 Watershed Sediment Fluxes

Annual sediment yields from the watershed that were used in the sediment dynamics model were quantified from the SWAT+ watershed model. The sediments were released to the hydrodynamic model through the watershed outlets that are presented in Figure 12 while the annual modeled sediment yield is shown in Figure 13.

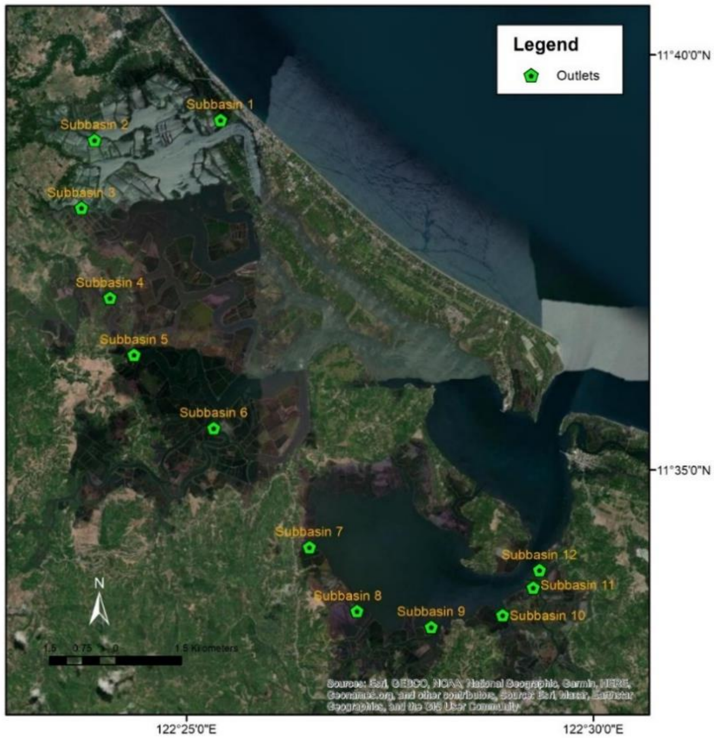

Figure 12. Watershed Outlets (Sediment Generation Points)

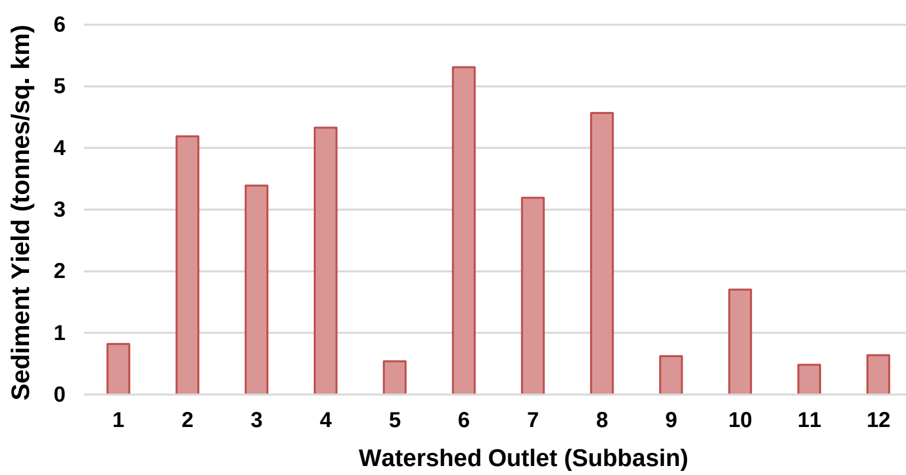

Figure 13. Model Simulated Annual Sediment Yield of Batan Bay Watershed

Outlets at subbasins having agricultural cover are found to have generated the largest average sediment yield. Although outlet 5 has the largest drainage area, much of the subbasin is covered with range lands thus being only the third largest source of sediments in the watershed. The drainage area of a subbasin affects the flow and sediment yields but the cover type also contributes largely on the amount of eroded sediments that will be transported to the streams.

A noticeable decrease in trend of agricultural areas can be seen from 1990 until 2010 while for range lands (brushes, grasslands, shrublands), the years 1990 to 2010 shows an increase in cover. At present (referring to year 2020), Batan Bay is still dominated by range lands covering about 58% of the watershed, followed by agriculture at 33%. Built-up areas have a generally increasing trend as a characteristic of growing population while the increase in aquaculture cover can also be attributed to the decrease in agricultural area, that is, a shift in livelihood of the residents.

Results of the simulated sediment yield from the watershed are based on calibrated discharges and its accuracy could further be improved by gathering field data on sediment discharge from the river outlets and performing model calibration. For this paper, the sediment dynamics model could still be improved after sediment discharge calibration and therefore would result in more accurate modelling of the sediment dynamics within the bay. But since the hydrodynamic parameters that affect the transport of the sediments were calibrated, the description of the transport if sediments are still acceptable for the objective of this study.

3.3 Tidal Flow Velocity

The study area is dominated by tides thus the flushing of water in and out of the bay follows the rhythmic fluctuation of tides. Figure 14 shows the current distribution in the bay during a flooding and ebbing. As shown in the figure, flows are generally stronger at entrance channels going to the central bay, to inner Batan Bay through the Pinamuk-an Channel and at the channel going to Tinagong Dagat. Strong velocities reaching up to 0.8 m/s are found at the mouth area where there is a sudden constriction upon entry or exit of the tide. The entrance channels as well as the channels around fishpond dikes tend to generate faster velocities.

Moreover, it can also be observed that there are faster velocities in channels between fishpond dikes and at entrance to these fishpond dikes. Identifying areas of high current magnitude and the corresponding current direction will be of useful information towards describing the sediment transport in the area.

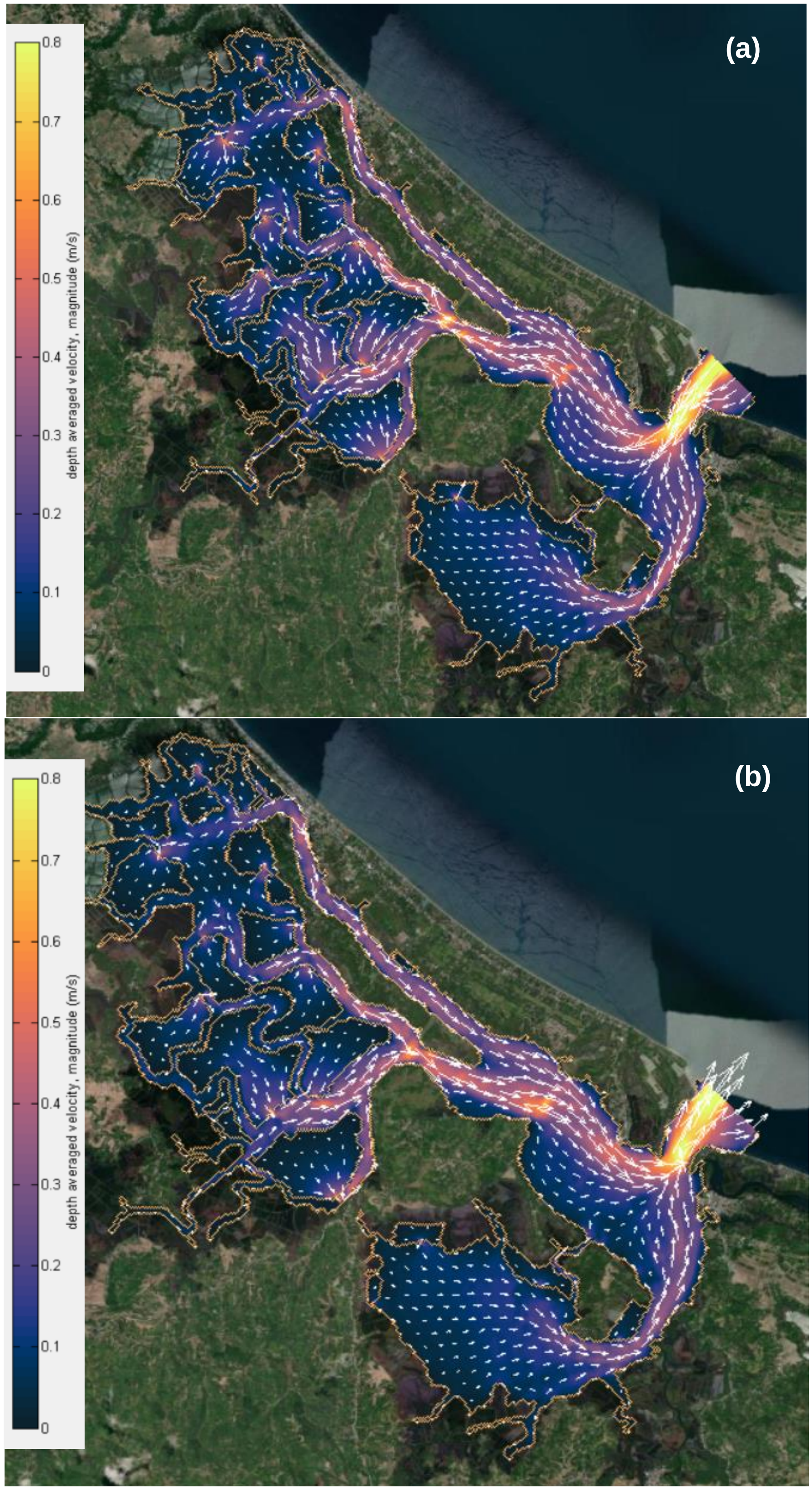

Figure 14. Current Distribution during (a) flood tide and (b) ebb tide

3.4 Sediment Transport and Morphological Changes

Fine sediments that are suspended in the water column could lead to increase in turbidity of waters that could affect other water quality parameters such as dissolved oxygen and temperature. This study will not include describing the water quality parameters mentioned but rather focus on the transport and movement of fine sediments that affect those parameters. Sediments are released in the bay through the watershed outlets. According to PAGASA, there are two major seasons in the Philippines: a dry season which runs from December to May and a wet season which runs from June to November. The seasonal fine sediment dynamics in Batan Bay is shown in Figure 15 where the dry season was represented by a timing in April where river discharges were low while the wet season was represented by a timing in October with higher river discharges.

During dry season, sediment dynamics is highly influenced by tidal motion where currents promote the suspension of fine sediments from the bed and resuspension of sediments in the water column. Higher fine sediment concentrations are found at channels around fishpond dikes and at and at other entrance channels going to the central and inner bay areas. These were also the areas that with higher velocity magnitudes as per described in the hydrodynamic results. Sediment concentrations ranging from 1.8 to 2.0 mg/L can also be noticed at entrances to fishpond dikes.

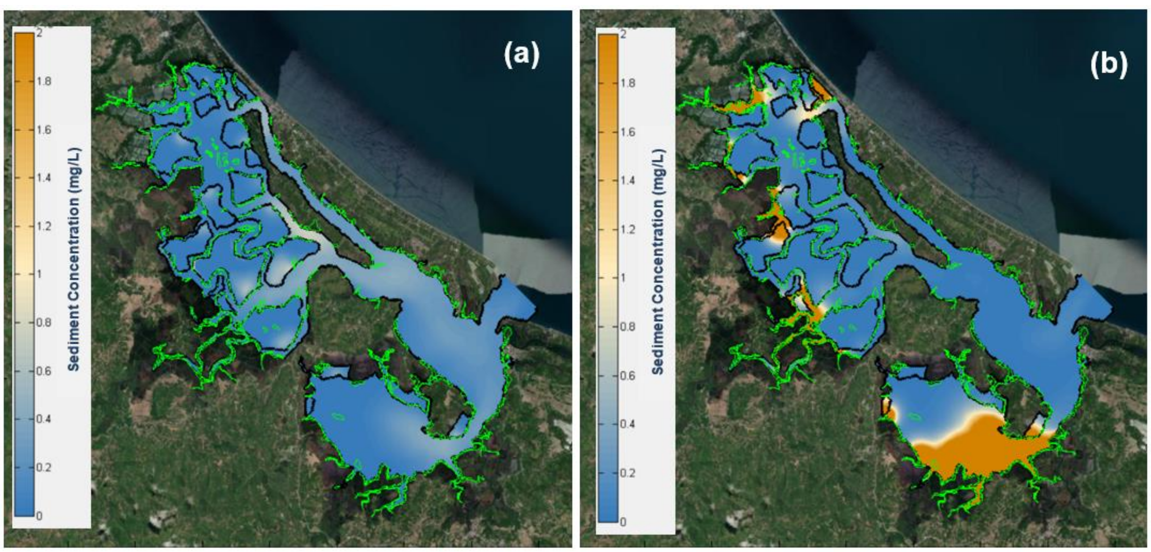

Figure 15. Fine Sediment Distribution During (a) Dry Season and (b) Wet Season

Fine sediment distribution and transport during the wet season is driven by yields from the watershed upstream. More freshwater discharges from the river delivering more sediments in the bay can be seen as high sediment concentrations are found near the watershed outlets. Although it can also be noticed that in the central and inner parts of the bay, dike structures affect the distribution of the sediments from the watershed since these structures tend to restrict the transport area for sediments to travel. As compared to the outlets that are discharging sediments in Tinagong Dagat, with the combined action of tides coming from the sea and fresh water from upstream, sediments are transported more easily.

Sediment concentrations showing sand, silt, and clay particles were also yielded by the sediment dynamics model. Figure 16 shows the sediment concentration at an observation point at Central Bay and in Tinagong Dagat. The bi-weekly sediment concentration pattern shows a highly fluctuating pattern can be observed both for the Central Bay and Tinagong Dagat observation stations. This can be attributed to the hydrodynamics of the bay where it is dominated by tides. Fluctuations of the sediment concentration follows the flooding and ebbing motion of the tides within the bay.

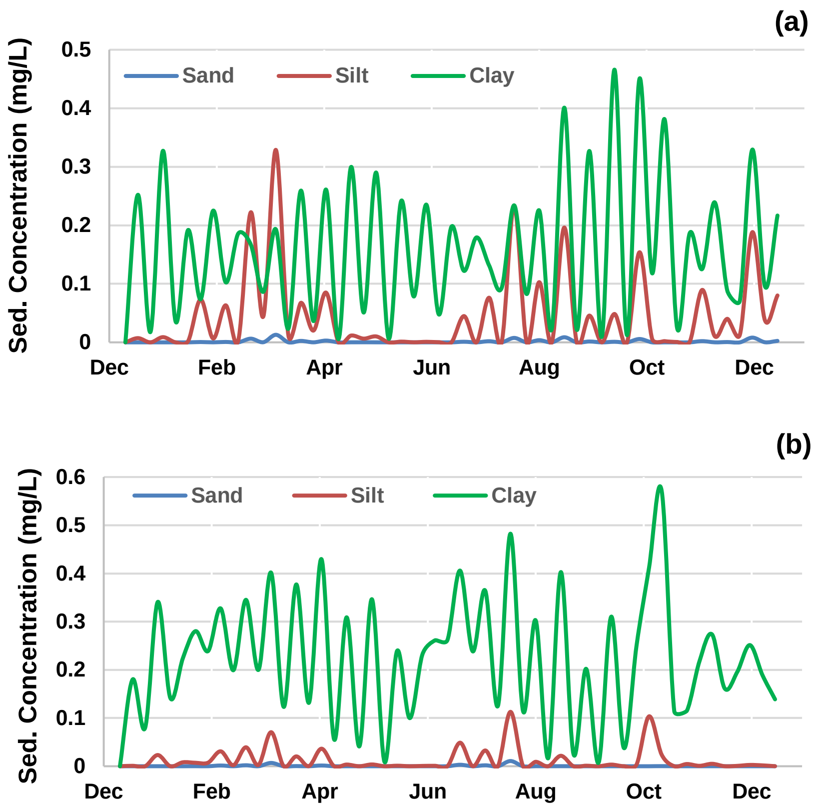

Figure 16. Time-series Sediment Concentrations at (a) Central Bay and (b) Tinagong Dagat

In addition, higher sediment concentrations can be observed during months of September to November that correspond to the wet season where an increase in sediments could have come from the watershed upstream and discharged into the bay.

Hydrodynamic simulations incorporating sediments also has the capability to capture and describe morphodynamic changes in an area. After a one-year simulation, areas of erosion and deposition were identified as shown in Figure 17 for Batan Bay and were related to the hydrodynamic results specifically the flow velocities and current directions.

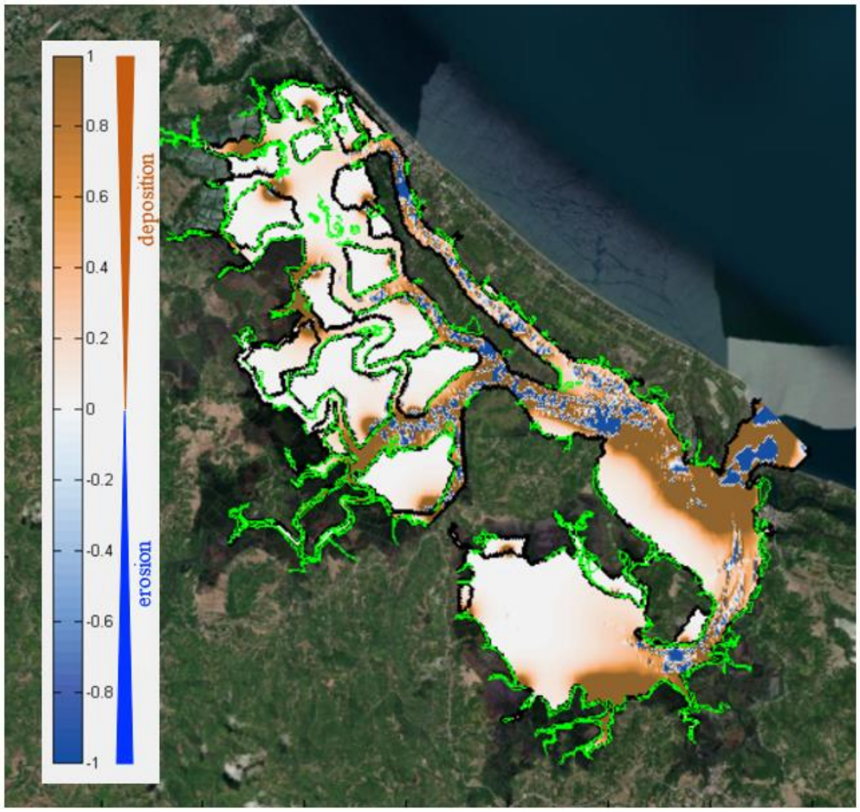

Figure 17. Cumulative Erosion and Deposition after a Year

Erosive areas that are shown at entrance channels can be attributed to the fast-moving currents that follow current direction during flooding and ebbing motion. Deposition can also be found at the entrances of the fishpond dikes as may have been transported by the action of the tides that move water in and out of the ponds. Moreover, channels near the watershed outlets tend to accumulate more sediments since the yields coming from the watershed are transported in these adjacent channels with respect to the direction of current during flood tide. Furthermore, based on the results of the sediment transport simulation, dike structures near watershed outlets hinder the transport of sediments thus causing more accumulation in those areas.

At the mouth of Batan Bay, erosion areas are also present which can be effects of the constriction at the entrance thus promoting faster velocities that go in and out of the bay. However, these areas show more deposition that covers a large area from mouth heading towards the entrance channels to the central and inner parts of the estuary. Based on the initial bathymetry that was presented in the prior section, these areas have depths ranging from 7 m to 10 m thus receiving sediments from currents that pass through this point during flooding and ebbing conditions. From the general distribution of erosion and deposition areas, it is evident that there are more areas of deposition than erosion that indicates shoaling for some parts of Batan Bay.

3.5 Model Application: Removing the Abandoned Fishponds

Fishpond dikes, just like any other structure, influences the hydrodynamics and sediment transport characteristic of the water body it is constructed on. Some of the fishpond dikes found in Batan Bay that were damaged by strong typhoons which passed through Aklan were no longer repaired. The ponds that are damaged by the strong typhoons and were not used anymore for aquaculture are referred in this paper as abandoned fishponds. This scenario was performed to assess the effects of removing these abandoned fishponds dikes on bay sediment dynamics and the resulting salinity distribution that is necessary for aquaculture activity. The fishpond dikes were modeled using thin dams in Delft3D which are depicted by the brown boundary lines in Figure 18. For this scenario, thin dams corresponding to the abandoned dikes were removed from the model domain and the location of abandoned fishponds that were removed for this scenario is also shown in the figure.

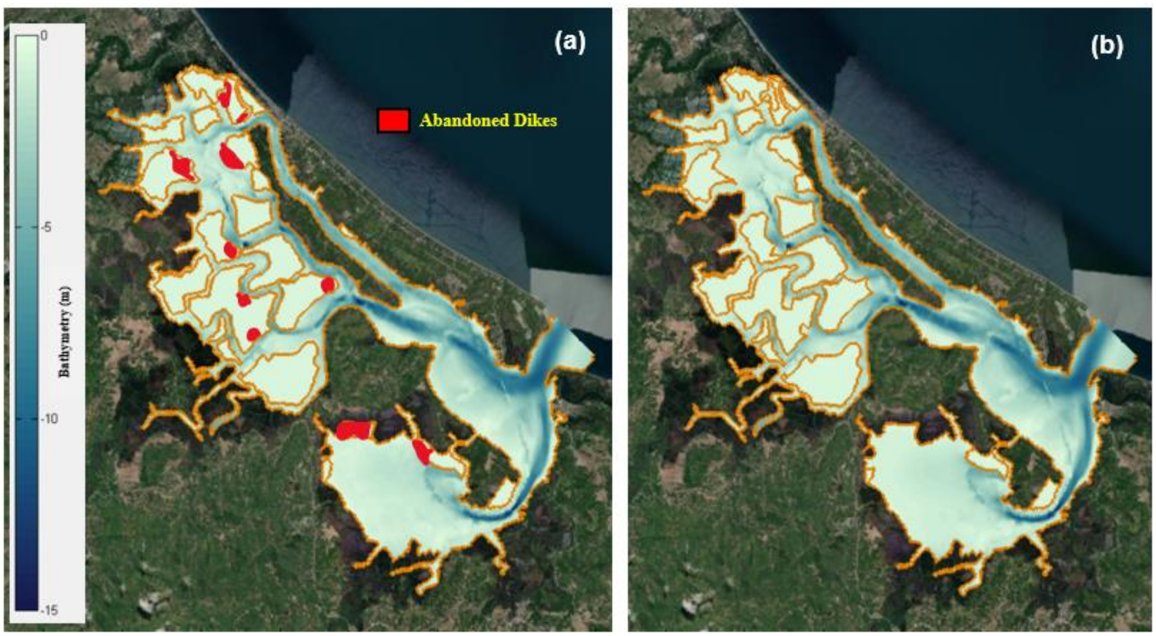

Figure 18. Model Domain Showing (a) Baseline Set-up with Location of Abandoned Fishponds for Removal and (b) After Removing Abandoned Ponds

3.5.1 Effects on Flow Velocity

A long-term (one-year) simulation was done, and the results were analyzed and compared with the baseline (present) condition of the bay. Shown in Figure 19 is the current distribution of Batan Bay before and after removing the abandoned fishpond dikes during the flood tide. There are faster moving flows near the areas of the removed fishpond dikes in addition to the usual areas of high velocity currents such as entrance channels and at the bay mouth. The removal of the abandoned dikes also meant removing the structure that impedes the flow of water, thus resulting to faster currents in these areas.

Also shown in Figure 19c is the difference between velocity magnitudes before and after removing the abandoned fishponds. As mentioned, areas near the removed dikes resulted in an increase in velocity by as much as 0.5 m/s. Moreover, the rest of the bay's current distribution has been maintained as shown by the zero difference in most parts of the study area.

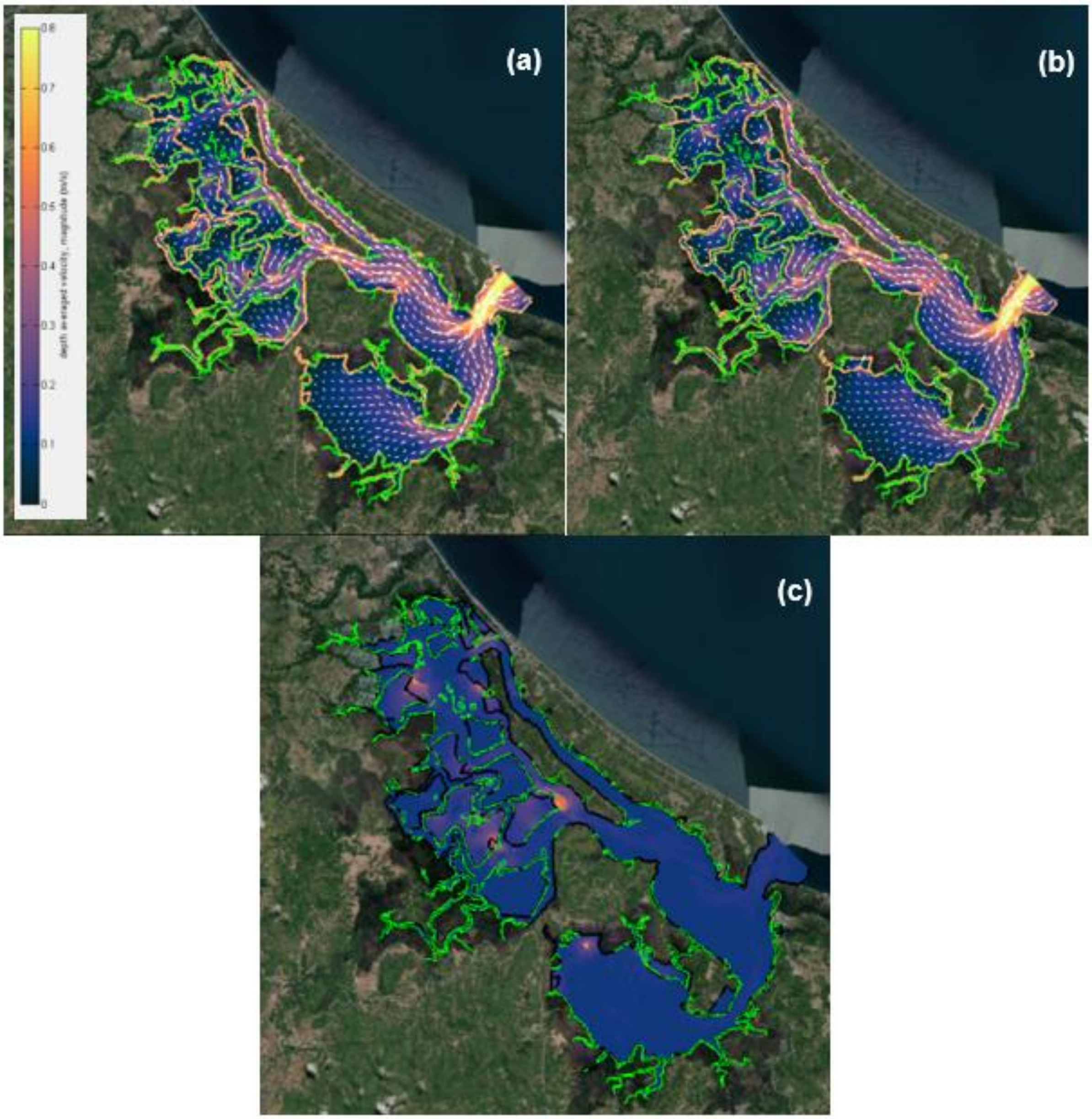

Figure 19. Current Distribution during Flood Tide for (a) Baseline (present), (b) After Removing the Abandoned Fishpond Scenario, and (c) Velocity Magnitude Difference

3.5.2 Effects on Erosion and Deposition Areas

As this paper aimed to describe the sedimentation dynamics of the bay, considering the effects of possible bay management scenarios in terms of erosion and deposition is necessary.

Shown in Figure 20 is the cumulative erosion and deposition in the Bay considering the removal of abandoned dikes after one year of sedimentation processes.

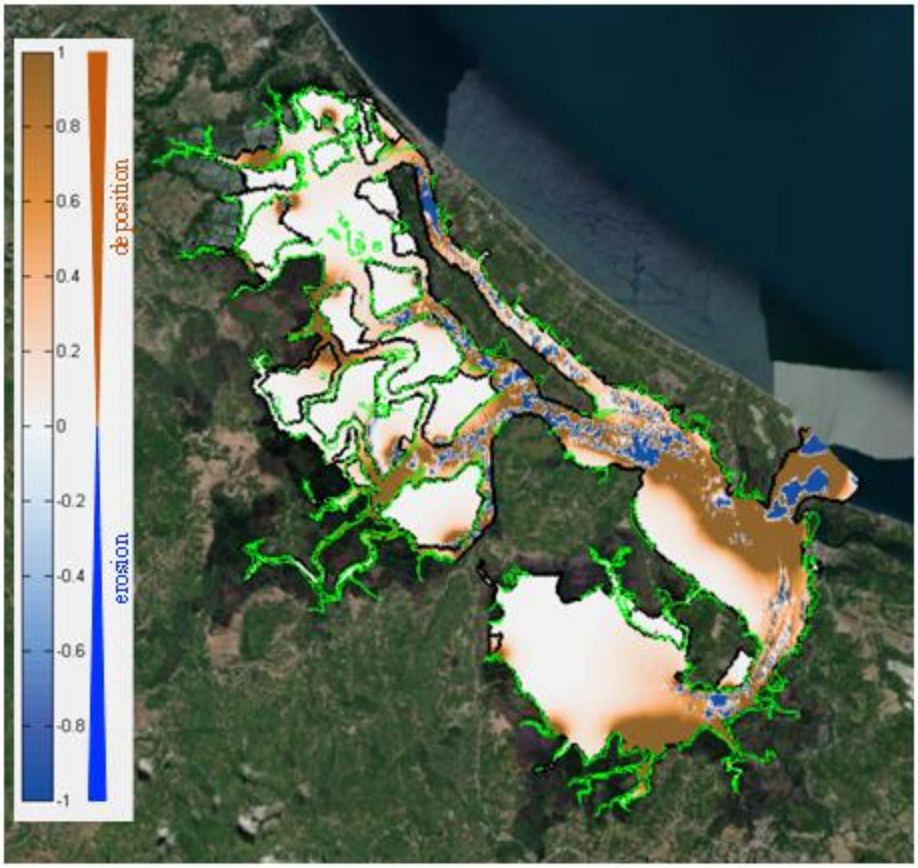

Figure 20. Cumulative Erosion and Deposition After Removing Abandoned Fishpond Dikes

Removing the fishpond dikes produced more erosion near these areas which can be caused by faster moving flows. Moreover, areas near the removed dikes were found to have less deposition in general as compared to the results of the baseline condition presented earlier. Areas near the watershed outlets still exhibit large depositions mainly due to receiving yields from upstream that are carried by the current.

The baseline condition after one year of simulation showed that the average increase in bed level (deposition) from the observation stations was found to have reached 1.99 cm while the decrease in bed level (erosion) was 2.25 cm at the average. Comparing the results to the scenario that removed the abandoned fishponds in terms of erosion and deposition areas after a year of simulation, map results show that there are more blue regions signifying less sediment deposition specifically in those channels where flow magnitudes are high. Less deposition could have been caused by the increase in area where sediment can be transported because of removing some of the dikes.

IV. CONCLUSIONS AND RECOMMENDATIONS

This study developed a hydrodynamics-sediment dynamics model to describe and understand the sedimentation features of Batan Bay in Aklan. Hydrological processes were discussed including current flow and sediment regime, as well as identifying major sources of upstream sediments. Hydrodynamic conditions of Batan Bay were also described including the sediment dynamics that was used to describe fine-sediment transport patterns and identify areas of erosion and deposition within the bay. The following conclusions were drawn from this study.

a. The sediment yield of Batan Bay watershed is influenced by the varying seasons, the existing topographical and landcover characteristics of the watershed as shown in the results of the watershed model.
b. Hydrodynamic model results indicate that the current distribution in the bay show faster moving flows at entrance channels same as with channels located between fishpond dikes and at entrance to the fishpond dikes.
c. Fine sediment transport pattern varies seasonally. During dry season, sediments are transported through the action of tides while much of the sediments transported during wet season come from the yields of the upstream carried out through the watershed outlets.
d. Using the developed sediment dynamics model, deposition areas were identified at fishpond dike entrances and near the bay mouth. Channels that are near watershed outlets were also found to have significant deposition while erosion areas were identified at the narrow channels between fishpond dikes with faster moving flows.
e. Removing abandoned fishponds in the bay as a possible management scheme was examined through model scenario analysis. An increase in the velocity magnitude by as much as 0.5 m/s were observed at areas near the removed structures.

Batan Bay in Aklan, an estuary driven by tides coming from the sea and river influx coming from the upstream watersheds, is a system with multiple drivers that affects the aquaculture ecosystem within the bay. With the aid of numerical models that were used in this study, the complex system of the study area was described and the information generated can aid local stakeholders towards promoting a more sustainable aquaculture development. Moreover, the effects on erosion or deposition of constructing new fishpond dikes within the bay could also be described using the sediment dynamics model that was used in this study. On the other hand, changes in flow and sediment flux brought about by future urbanization upland can also be studied using the watershed model that was set-up in this study.

The results generated from the models can aid the community in understanding the effects of their future developments on the sedimentation dynamics within the bay. However, obtaining hydrologic field data such as observed river discharges could help improve further the watershed model in simulating the discharges of the river outlets that drain to Batan Bay. The hydrodynamic model in Delft3D on the other hand can also be modified by representing the fishpond dikes in a fully-closed condition and assessing its effects on the hydrodynamics and sediment dynamics of the bay. In addition, obtaining field sediment data such as the fundamental sediment properties through core sampling and sediment concentrations for validation of the watershed sediment yield can give a much better representation of sediment behavior of the study area. Furthermore, collecting spatio-temporal data on sediment concentrations for setting up a more defined initial and boundary condition could be of aid in the calibration and validation of the sediment dynamics model. Lastly, the outputs of this current work can be improved further by conducting sensitivity analysis on the parameters that pertain to sediment behavior such as settling velocity and sediment concentration for a more accurate description of the sediment dynamics of the site toward science-based decision support information for bay conservation and management.

V. ACKNOWLEDGEMENTS

This study was made possible through the funding of the Japan International Cooperation Agency (JICA) and the National Hydraulics Research Center (NHRC) through the Comprehensive Assessment and Conservation of Blue Carbon Ecosystems and their Services in the Coral Triangle (BlueCARES) Project.

References:

[1] Gusmawati NF, Zhi C, Soulard B, Lemonnier H, Selmaoui-Folcher N. 2016. Aquaculture pond precise mapping in Perancak Estuary, Bali, Indonesia. J Coast Res. 1(75):637–641. doi: 10.2112/SI75-128.1

[2] Ottinger M, Clauss K, Kuenzer C. 2017. Large-scale assessment of coastal aquaculture ponds with Sentinel-1 time series data. Remote Sens (Basel). 9(5). doi: 10.3390/rs9050440

[3] Pokavanich T, Guo X. 2024. Saltwater intrusion in Chao Phraya Estuary: A long, narrow and meandering partially mixed estuary influenced by water regulation and abstraction. J Hydrol Reg Stud. 52. doi: 10.1016/j.ejrh.2024.101686

[4] Schulz E, Grasso F, Le Hir P, Verney R, Thouvenin B. 2018. Suspended sediment dynamics in the Macrotidal Seine Estuary (France): 2. Numerical modelling of sediment fluxes and budgets under typical hydrological and meteorological conditions. J Geophys Res Oceans. 123(1):578–600. doi: 10.1002/2016JC012638

[5] Reisinger A, Gibeaut JC, Tissot PE. 2017. Estuarine suspended sediment dynamics: Observations derived from over a decade of satellite data. Front Mar Sci. 4(DEC). doi: 10.3389/fmars.2017.00233

[6] Ha HK, Park K. 2012. High-resolution comparison of sediment dynamics under different forcing conditions in the bottom boundary layer of a shallow, micro-tidal estuary. J Geophys Res Oceans. 117(6): 1–14. doi: 10.1029/2012JC007878

[7] Garel E, Pinto L, Santos A, Ferreira Ó. 2009. Tidal and river discharge forcing upon water and sediment circulation at a rock-bound estuary (Guadiana estuary, Portugal). Estuar Coast Shelf Sci. 84(2):269–281. doi: 10.1016/j.ecss.2009.07.002

[8] Werllen J, Azevedo DJ, Carlos A, De Castro L. 2016. Siltation rate and main anthropic impacts on sedimentation of the São Luís tidal inlet - State of Maranhão, Brazil. 64(1):9–18.

[9] Lomborg U, Pejrup M. 2005. Modelling of cohesive sediment transport in a tidal lagoon — an annual budget. 218:1–16. doi: 10.1016/j.margeo.2005.03.015

[10] Bastos L, Bio A, Iglesias I. 2016. The importance of marine observatories and of RAIA in particular. 3: August:1–11. doi: 10.3389/fmars.2016.00140

[11] Cheng Z, Jalon-Rójas I, Wang XH, Liu Y. 2020. Impacts of land reclamation on sediment transport and sedimentary environment in a macro-tidal estuary. Estuar Coast Shelf Sci. 242. doi: 10.1016/j.ecss.2020.106861

[12] Wang XH, Andutta FP. 2013. Sediment transport dynamics in ports, estuaries and other coastal environments. p. 2–3.

[13] Defne Z, Ganju NK, Moriarty JM. 2019. Hydrodynamic and morphologic response of a back-barrier estuary to an extratropical storm. J Geophys Res Oceans. 124(11):7700–7717. doi: 10.1029/2019JC015238
[14] Beudin A, Kalra TS, Ganju NK, Warner JC. 2017. Development of a coupled wave-flow-vegetation interaction model. Comput Geosci. 100:76–86. doi: 10.1016/j.cageo.2016.12.010
[15] Warner JC, Sherwood CR, Signell RP, Harris CK, Arango HG. 2008. Development of a three-dimensional, regional, coupled wave, current, and sediment-transport model. Comput Geosci. 34(10): 1284–1306. doi: 10.1016/j.cageo.2008.02.012
[16] Lesser GR, Roelvink JA, van Kester JATM, Stelling GS. 2004. Development and validation of a three-dimensional morphological model. Coastal Engineering. 51(8–9)883–915. doi: 10.1016/j.coastaleng.2004.07.014
[17] Ton AM, Vuik V, Aarninkhof SGJ. 2023. Longshore sediment transport by large-scale lake circulations at low-energy, non-tidal beaches: A field and model study. Coastal Engineering. 180. doi: 10.1016/j.coastaleng.2022.104268
[18] Ghareeb M, Salama R, ElSherbini S. 2023. Impact of the sustainable waterfront proposed development of Bani-Suif corniche on the hydraulics of the Nile River. Ain Shams Engineering Journal. 14(1). doi: 10.1016/j.asej.2022.101845
[19] Boudet L, Sabatier F, Radakovitch O. 2017. Modelling of sediment transport pattern in the mouth of the Rhone Delta: Role of storm and flood events. Estuar Coast Shelf Sci. 198: 568–582. doi: 10.1016/j.ecss.2016.10.004
[20] Tu LX, *et al.* 2019. Sediment transport and morphodynamical modelling on the estuaries and coastal zone of the Vietnamese Mekong Delta. Cont Shelf Res. 186:64–76. doi: 10.1016/j.csr.2019.07.015.
[21] Dykes J, Allard RA, Kaihatu JM. 2006. Evaluation of Delft3D performance in nearshore flows arctic data assimillation view project tidal stream site characterization view project.
[22] Ikejima K, Ronquillo JD, Corre VL, Dureza VA. 2006. Fish assemblages in abandoned ponds and waterways surrounding brackish water aquaculture ponds in Panay Island, the Philippines. Asian Fish Sci. 19:293–307.
[23] Altamirano J, Kurokura H, Salayo ND, Baticados D, Suyo JG, Ishikawa S. 2014. Community-based shrimp stock enhancement for coastal socio-ecological restoration in the Philippines. Resource enhancement and sustainable aquaculture practices in Southeast Asia: challenges in responsible production of aquatic species. International workshop on resource enhancement and sustainable aquaculture practices in Southeast Asia. p. 159–167.
[24] Hawker L, Bates P, Neal J, Rougier J. 2018. Perspectives on Digital Elevation Model (DEM) simulation for flood modelling in the absence of a high-accuracy open access global DEM. Front Earth Sci (Lausanne). 6. doi: 10.3389/feart.2018.00233
[25] Puno GR, Puno RCC, Maghuyop IV. Flood hazard simulation and mapping using digital elevation models with different resolutions. Global Journal of Environmental Science and Management. 8(3):339–352. doi: 10.22034/gjesm.2022.03.04
[26] User Manual. Delft3D 3D/2D modelling suite for integral water solutions Hydro-Morphodynamics.
[27] Bautista D, Herrera E, Hernandez B, Yoshikai M, Nakamura T, Nadaoka K. 2020. Numerical investigation of coastal sediment transport for assessment of coastal erosion of a Philippine coastline using a 3D hydrodynamic model. IOP Conf Ser Mater Sci Eng. 849(1):0–15. doi: 10.1088/1757-899X/849/1/012091
[28] Mcknight K, Lowe J, Plane E. 2020. Special study on bulk density final report.
[29] Pearson SG, et al. 2021. Characterizing the composition of sand and mud suspensions in coastal and estuarine environments using combined optical and acoustic measurements. J Geophys Res Oceans. 126(7). doi: 10.1029/2021JC017354
[30] Wang YP, et al. 2013. Sediment resuspension, flocculation, and settling in a macrotidal estuary. J Geophys Res Oceans. 118(10):5591–5608. doi: 10.1002/jgrc.20340
[31] Dile YT, Daggupati P, George C, Srinivasan R, Arnold J. 2016. Introducing a new open source GIS user interface for the SWAT model. Environmental Modelling and Software. 85: 129–138 doi: 10.1016/j.envsoft.2016.08.004
[32] Delft3D flexible Mesh suite 1D/2D/3D Modelling suite for integral water solutions User Manual RGFGRID.
[33] Rijn LC van. 1993. Principles of sediment transport in rivers, estuaries and coastal seas. Aqua Publications. The Netherlands.

[34] Williams JJ, Esteves LS. 2017. Guidance on setup, calibration, and validation of hydrodynamic, wave, and sediment models for shelf seas and estuaries. Advances in Civil Engineering. Hindawi Limited. doi: 10.1155/2017/5251902

[35] Moriasi DN, Gitau MW, Pai N, Daggupati P. 2015. Hydrologic and water quality models: Performance measures and evaluation criteria. Trans ASABE. 58(6):1763–1785. doi: 10.13031/trans.58.10715

[36] Huang G-H. 2010. Measure of Association. International Encyclopedia of Education. Elsevier, Oxford. 7:260-263.

[37] Jamilla JM, Serrano J, Hernandez BC, Herrera E. 2021. Assessing the hydrologic effects of urbanization through numerical modelling using swat: A case study of Laguna de Bay basin. International Archives of the Photogrammetry, Remote Sensing and Spatial Information Sciences - ISPRS Archives. International Society for Photogrammetry and Remote Sensing. p. 193–199. doi: 10.5194/isprs-Archives-XLVI-4-W6-2021-193-2021